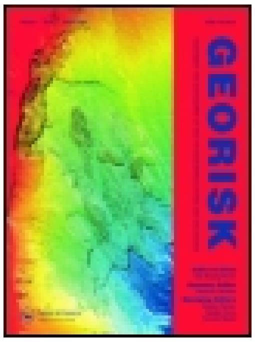

Taylor & Francis
Taylor & Francis Group

Georisk: Assessment and Management of Risk for Engineered Systems and Geohazards

ISSN: 1749-9518 (Print) 1749-9526 (Online) Journal homepage: http://www.tandfonline.com/loi/ngrk20

Assessing the influence of morpho-structural setting on landslide abundance

Ivan Marchesini, Michele Santangelo, Fausto Guzzetti, Mauro Cardinali & Francesco Bucci

To cite this article: Ivan Marchesini, Michele Santangelo, Fausto Guzzetti, Mauro Cardinali & Francesco Bucci (2015): Assessing the influence of morpho-structural setting on landslide abundance, Georisk: Assessment and Management of Risk for Engineered Systems and Geohazards, DOI: 10.1080/17499518.2015.1058956

To link to this article: http://dx.doi.org/10.1080/17499518.2015.1058956

Published online: 14 Sep 2015.

Georisk, 2015
http://dx.doi.org/10.1080/17499518.2015.1058956

Assessing the influence of morpho-structural setting on landslide abundance

Ivan Marchesini, Michele Santangelo*, Fausto Guzzetti, Mauro Cardinali and Francesco Bucci

Istituto di Ricerca per la Protezione Idrogeologica, Consiglio Nazionale delle Ricerche, Perugia 06128, Italy

(*Received 7 January 2015; accepted 31 May 2015*)

Knowing the factors that influence landslide abundance and distribution is important to evaluate landslide susceptibility and hazard. Visual interpretation of aerial photographs (API) can be used to collect spatially distributed information on bedding attitude (BA), in an area. Where a map of the location of bedding traces (BTs), i.e. lines showing the intersection of bedding planes with the local topography, is available, the map can be used to obtain BA point data and to prepare maps showing morpho-structural domains. The possibility of using BA maps to investigate the influence of morpho-structural settings on landslide abundance is hampered by the lack of understanding of the influence of the length of the BTs, and of the parameters used to interpolate the BA data on the structural zonation. To investigate the problem, we used information on 207 BTs obtained through API in the Collazzone area, Central Italy, and we prepared 150 maps showing BA information. This was accomplished using 15 different values for the segmentation length of the BTs (S), and 10 different values for the tension parameter (T) used for the interpolation. We compare the results against previous results obtained for the same area adopting a heuristic approach to the segmentation of the same set of BTs. Next, we compare the geographical distribution of old deep-seated, deep-seated and shallow landslides in five morpho-structural domains in the study area, and we analyse the influence of the structural settings on the abundance of the different types of landslides.

Keywords: bedding domain; structure; landslide; validation

1. Introduction

Empirical evidence indicates that geological discontinuities, including bedding, foliation, faults, joints and cleavage systems, condition the distribution and abundance of landslides (Guzzetti, Cardinali, and Reichenbach 1996; Günther 2003; Goudie 2004; Grelle et al. 2011; Bucci, Cardinali, and Guzzetti 2013). Inspection of the literature reveals that only a few attempts were made to exploit bedding attitude (BA) data (or similar geometric data for other geological discontinuities) in regional analyses of landslide distribution, or for landslide susceptibility or hazard modelling (Marchesini et al. 2014; Mergili et al. 2014b). A reason for the shortage of applications is the difficulty in the treatment of the BA data. BA data are commonly collected through geologic field surveys (Clegg et al. 2006; De Donatis and Bruciatelli 2006; Bodien and Tipper 2013) and stored as circular point information. The BA point data suffer from heterogeneity in their spatial density and need to be interpolated to obtain spatially distributed information on local bedding geometry (attitude). The interpolation of BA point data is further hampered by the fact that directional data cannot be interpolated simply (e.g., De Kemp 1998; Grelle et al. 2011; Santangelo et al. 2014).

Recently, Marchesini et al. (2013) and Santangelo et al. (2014) have proposed an approach to prepare spatially distributed maps of BA exploiting information gathered from the visual interpretation of stereoscopic aerial photographs (API) to obtain BA point data and interpolating the point data to prepare maps showing the dip direction and inclination of the bedding. The BA maps are then used in combination with a Digital Elevation Model (DEM) to determine the geometric relationship between the BA and the local slope. This allows preparing maps portraying morpho-structural domains, including anaclinal, orthoclinal and cataclinal slopes.

The approach is in five steps (Santangelo et al. 2014). First, API is used to identify and map single "bedding traces" (BTs), which are linear signatures left by layered rocks on the topographic surface (Santangelo et al. 2014). Next, the individual BTs are "draped" on a digital topography represented by a DEM, and the inclination and dip direction of the "best-fitting planes" of each three-dimensional BT is determined. Next, for each BT, the geometric point representing the BA of the best-fitting plane is placed in the centre of the bounding box encompassing the BT, and information on the dip direction and

*Corresponding author. Email: michele.santangelo@irpi.cnr.it

inclination of the best-fitting plane is associated to the central point. Next, the BAs are considered unit vectors represented by their components (EW, NS and vertical), and the three components are interpolated geographically. The three resulting raster layers are used to prepare maps of the bedding inclination and dip direction. Finally, the raster maps, with maps showing terrain slope and aspect obtained from the DEM, and a map showing the TOpographic Bedding plane Intersection Angle (TOBIA) index of Meentemeyer and Moody (2000), are used to determine the morpho-structural domains.

In their work, Santangelo et al. (2014) have not investigated the influence of the length of the individual BTs, and of the parameters used for the geographical interpolation of the BA point data, on the determination of the morpho-structural domains. BTs are of variable lengths, depending on the topographic and morphological signature of the intersection of the bedding plane with the local topography. The ability of an interpreter to visually detect and map the signature of the single BTs in the aerial photographs influences significantly the length of the BTs. Landslide and debris deposits, the presence of forest and of other land cover types, and human-induced terrain modifications can interrupt the (visual) continuity of the BTs, limiting the ability to recognize them and constraining their length. Selection of the appropriate interpolation algorithm, and of the proper values for the parameters adopted for the geographical interpolation of the BA point data, also affects the definition of the morpho-structural domains. For their interpolation, Santangelo et al. (2014) used a regularized spline with tension and smoothing (RST) algorithm (Mitášová, Mitášm, and Harmon 2005; Neteler and Mitášová 2008). In the algorithm, the (non-dimensional) tension parameter (T) is decided a priori and controls the distance over which each BA point measurement influences the interpolated surface. Large values of the tension parameter weight more heavily nearby measurement points, and small values of the tension parameter weight more points located at larger distances. Selection of the "optimal" value for the tension parameter remains an open problem (Hofierka, Cebecauer, and Šúri 2007).

An additional factor conditioning the quality of the geographical interpolation of the BA point data obtained through API consists in determining how to maximise the information of each BT. A single (standard) procedure to decide the optimal length of the BTs does not exist. This is because the decision depends on multiple factors, including the local topography, the geological setting, the quality and resolution of the DEM, and the accuracy of the geographical location of the points representing the BTs on a topographic map. A photo-interpreter may decide to split (or not split) relatively long BTs, considering each segment of a BT representative of the local attitude of a single bedding plane. This has the advantage of increasing the number of the BAs that can be calculated from the same set of BTs, and of obtaining BA planes (and the corresponding dip directions and inclinations) that represent more accurately the local geometry of the bedding. However, a long BT can be segmented into smaller segments provided that the resulting segments are not straight. Straight (or nearly straight) segments cannot be used to fit a single plane. Moreover, due to local inconsistencies between the geographic location of the BTs and the DEM, the estimated BAs can be inaccurate, locally. Using longer BTs reduces the inconsistencies.

To maximize the use of the information provided by the BTs, Santangelo et al. (2014) adopted a heuristic approach based on photo-geomorphological criteria to split 207 original photo-interpreted BTs into a total of 223 BTs. However, an analysis of the impact of the heuristic segmentation of the BTs on the resulting map showing morpho-structural domains was not performed. This analysis is important because the quality of a morpho-structural domains map obtained from BA point data depends largely on the number of the BT segments, conditioned by the segmentation process. We acknowledge that the quality of a morpho-structural domains map depends also on other factors, including the abundance, quality and geographical distribution of the original BA point data, and the values of the tension parameter (T) used for their geographical interpolation.

In this paper, we analyse how the segmentation of the BTs and the value of the tension parameters used for the geographical interpolation affect the resulting morpho-structural domain map. We also investigate how to define an optimal ("best") combination of the parameters that maximise the morpho-structural information captured through the API to define the geometrical relationships between the local morpho-structural setting and the abundance of landslides of different types.

2. Study area and data

We performed our experiment in the Collazzone area, Umbria, Central Italy (Figure 1). Elevation in the area ranges between 145 m along the Tiber River flood plain and 634 m at Monte di Grutti. Landscape is hilly, and lithology and the attitude of bedding planes control the morphology of the slopes. Lithology

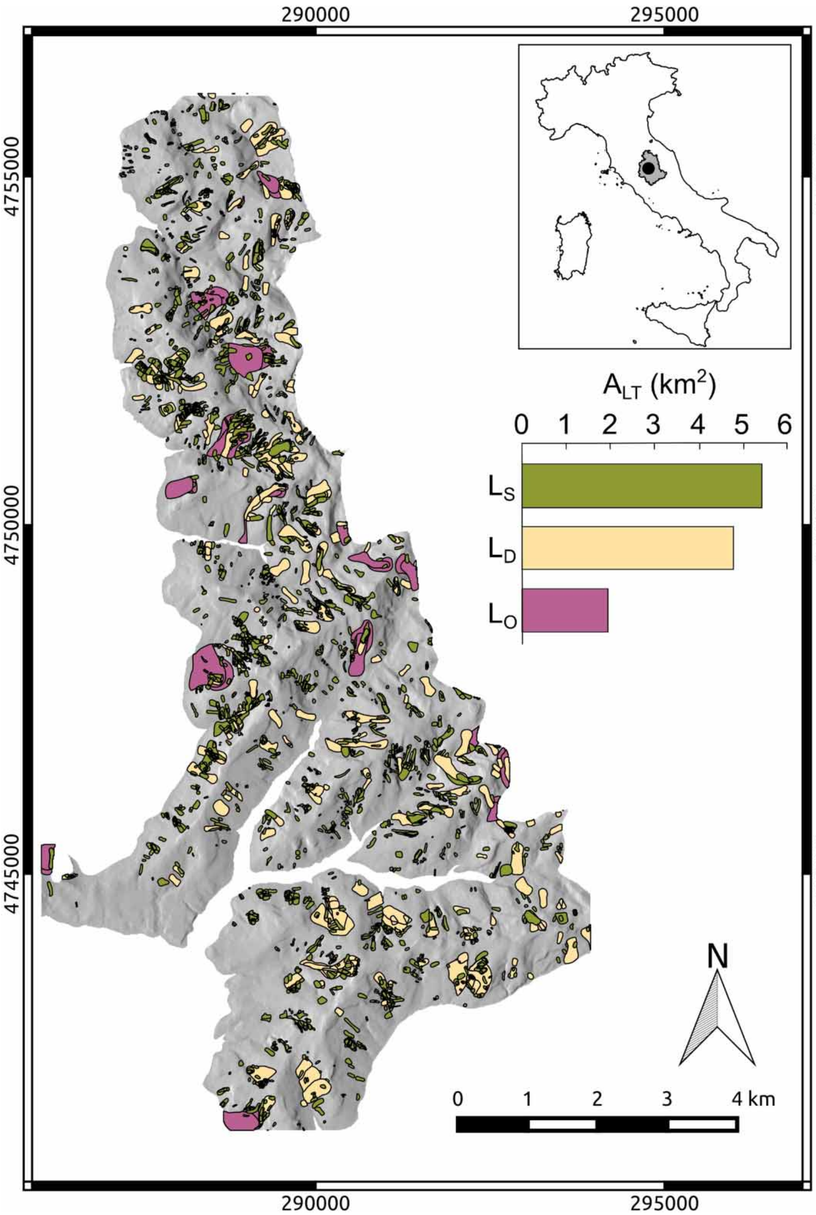

Figure 1. Multi-temporal landslide inventory map for the Collazzone area, Umbria, Central Italy. Histogram shows legend and total landslide area, ALT (in km^2) for three landslide classes. L_S, shallow landslide; L_D, deep-seated landslide; L_O, old deep-seated landslide. Shaded relief image obtained illuminating from NW a 10 m × 10 m DEM. UTM zone 33, datum ED50 (EPSG: 23033).

is represented by alternating layers of continental sediments composed of gravel, sand and clay (for a detailed description of the lithology in the study area, see Mergili et al. 2014a, 2014c). The thickness of the lithological layers and their mechanical properties control their morphological appearance and visual evidence in the landscape. The structural setting is regular, with gently dipping bedding organized in a broad syncline. With this respect, the lithological and structural settings are ideal to experiment the interpolation of BA point data.

A 10 m × 10 m DEM obtained interpolating 5 and 10 m contour lines was available to us, together with a multi-temporal landslide inventory map obtained through the interpretation of multiple sets of aerial photographs, and detailed geological and geomorphological field surveys (Figure 1; Guzzetti et al. 2006, 2009; Fiorucci et al. 2011). The inventory shows 1785 landslides grouped in three broad classes, including old deep-seated landslides (L_O), deep-seated landslides (L_D) and shallow landslides (L_S). The subdivision was based on the information on the estimated age, depth and type of movement stored in the geographical landslide database (Guzzetti et al. 2006, 2009; Fiorucci et al. 2011).

In the inventory, L_O are 16 large slides and slide earthflows with an average landslide area of AL = $1.7 \times 104\ \mathrm{m}^2$. These are dormant, old or relict landslides (Keaton and DeGraff 1996) dismantled by erosion. Their location and geometry suggest a control of lithology, structure and the local attitude of bedding planes on the location, geometry and size of the landslides (Santangelo et al. 2014). Where known, the sliding surface of L_O is > 10 m in depth. L_D and L_S are dormant, mature, active or recently active landslides (Keaton and DeGraff 1996). L_D include 258 slides, slide earthflows and complex landslides with an average landslide area of AL = $2.5 \times 104\ \mathrm{m}^2$. Although distinction between L_D and L_O was difficult, locally, L_D are less dismantled by erosion and are less modified by more recent failures than the L_O. Where known, the sliding surface of L_D is in the range of 5 and 15 m. L_S include 1511 shallow landslides, mostly slide and flow-type movements, with $1.0 \times 102 < \mathrm{AL} < 2.8 \times 104\ \mathrm{m}^2$. The sliding surfaces of L_S are shallower than 5 m, and

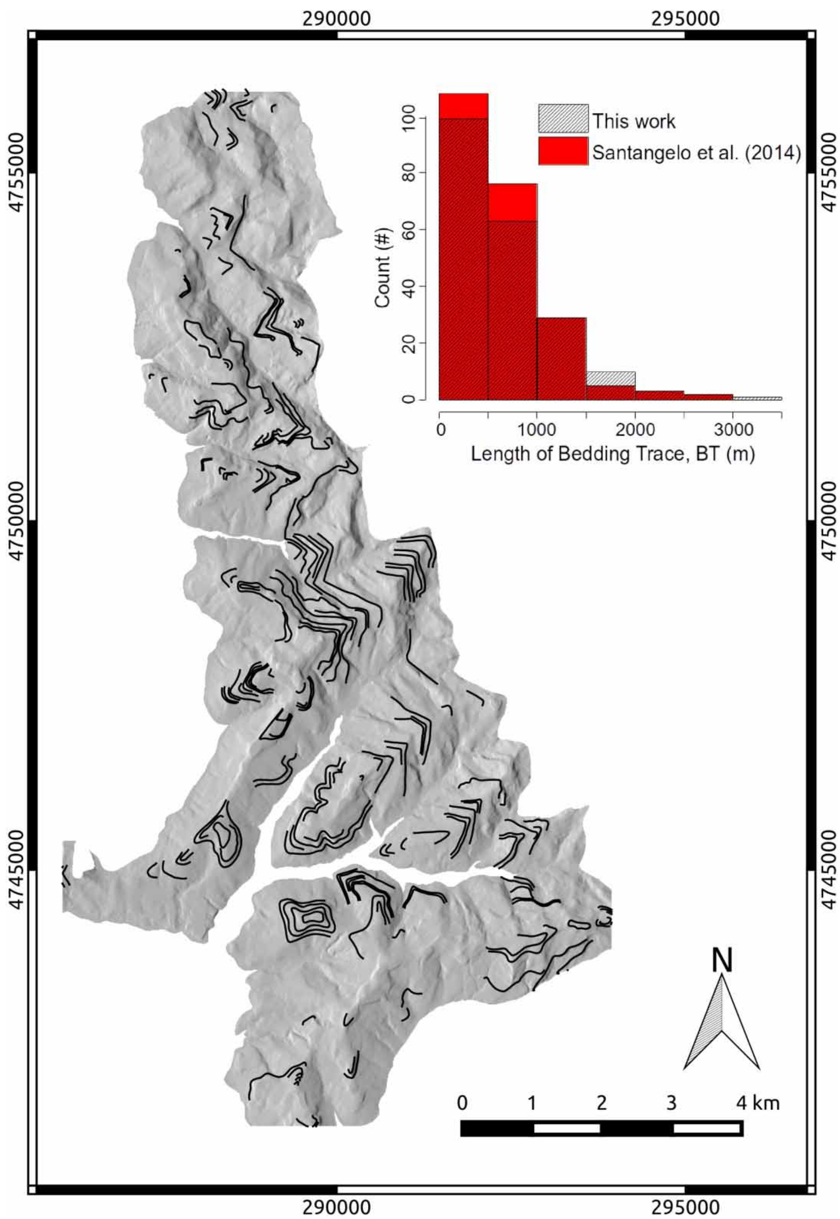

Figure 2. Map showing 207 bedding traces (BTs, black lines) obtained by visual interpretation of stereoscopic aerial photographs. Histogram compares the distribution of the 207 BTs used in this work (red bars) with the distribution of 223 BTs used by Santangelo et al. (2014) (hachured bars) for the same area. UTM zone 33, datum ED50 (EPSG: 23033).

most commonly 1.5 m in depth (Fiorucci et al. 2011; Mergili et al. 2014c).

For our work, we used the same 207 BTs used by Santangelo et al. (2014). In their original work, the longest BTs (around three km) were segmented based on a heuristic interpretation made by the same expert interpreter who completed the geomorphological mapping. The segmentation resulted in 223 BTs. In this work, we first considered the 207 original BTs, without any further segmentation. Figure 2 shows the count of the segmented (Santangelo et al. 2014) and the original, non-segmented (this work) BTs, for different lengths.

3. Method

To verify the impact of the segmentation of the BTs on the resulting morpho-structural domains map, we segmented all the BTs in the original data set (Figure 2) using different segmentation lengths, decided arbitrarily. We prepared a total of 15 maps of the BTs where, for each map, the maximum length of each segment S did not exceed a selected length, ranging from $S = 200$ m to $S = 3000$ m, in 200 m steps. Subsequently, for each map of the BTs obtained using a maximum value of S, all the segments with a sinuosity (Lisle 1996) $s \leq 1.01$ were identified and discarded. Sinuosity was defined as the ratio between the length of a segment and the length of the straight line connecting the end points of the same segment. A value of $s = 1.01$ was selected arbitrarily to identify (and exclude) straight or nearly straight segments through which a single-fitting plane cannot be fitted accurately. Then, for each of the 15 maps we obtained corresponding maps showing the geographical distribution of the BA using the approach proposed by Marchesini et al. (2013).

Geographical interpolation of the BA was performed considering separately the three components of the unit vector perpendicular to the bedding plane described by the BA data (Santangelo et al. 2014). The three resulting maps of the BA components were then recombined to obtain two maps showing the (1) bedding inclination and (2) dip direction. In their work, Santangelo et al. (2014) adopted a RST algorithm (Mitášová, Mitášm, and Harmon 2005; Neteler and Mitášová 2008) for the geographical interpolation of the BA point data and selected a tension value $T = 40$. In this work, to investigate the influence of the tension value T on the morpho-structural domains maps, the single BAs maps were interpolated using 10 different tension values (i.e. from $T = 10$ to 100, with steps of 10). The range was selected because experience indicates that suitable values for the parameter T are in the range $10 \leq T \leq 100$ and do not depend on the actual scale (distance) of the original data (see v.surf.rst manual, GRASS GIS development team, 2015). The tension parameter T acts as a rescaling factor for the distance between the location of the grid cell where the interpolated value is computed and the location of the measurement point data. A low tension increases the role of the distant points, and a large tension reduces the effect of the distant points.

To determine the optimal combination between the maximum length of the segmentation S and the value of the interpolation parameter T, we adopted a cross-validation procedure for each combination of the two variables. We tested 450 maps (15 different segmentation lengths, 10 different values of T and three components of the BAs). For the cross-validation, we adopted a "jack-knife" approach (Hofierka et al. 2002) and, for each map, we removed one input measurement data point and performed the interpolation at the location of the removed point using the remaining measurement points. The difference between the original measurement data point and the interpolated value was estimated, and the performance of the interpolation was measured by the mean absolute error (MAE).

Combining the values of the MAE calculated in the EW, NS and the vertical directions, we obtained the magnitude (modulus) of the mean vector of the error, for each of the 150 interpolated maps (15 different values of S and 10 different values of T). We used this value to select the optimal ("best") combination of the size for the segmentation S and the value of the tension T to be used for the "optimal" modelling of the BA in our study area. Next, we used the "optimal" combination to prepare a map of the morpho-structural domains (Santangelo et al. 2014) and to analyse the influence of the different domains on the geographical occurrence and abundance of landslides of different types.

4. Results

Analysis of the results of the segmentation process indicates that increasing the number of the BT segments (using a shorter segmentation length S) does not increase the number of significant BA point measurement data, necessarily. Adopting a segmentation length $S = 200$ m, we obtained a total of 817 BTs segments, of which 555 with a sinuosity $s > 1.01$ were retained for the analysis. In our experiment, the number of BT segments with $s \leq 1.01$ (i.e. the segments that were excluded) decreased with increasing S and reduced to zero for $S = 1200$ m.

Figure 3 shows the results of the cross-validation using the MAE, for the three components (EW, NS and vertical) of the unit vector representing a BA data point, and for 450 combinations of the tension T and the segmentation length S parameters. Inspection

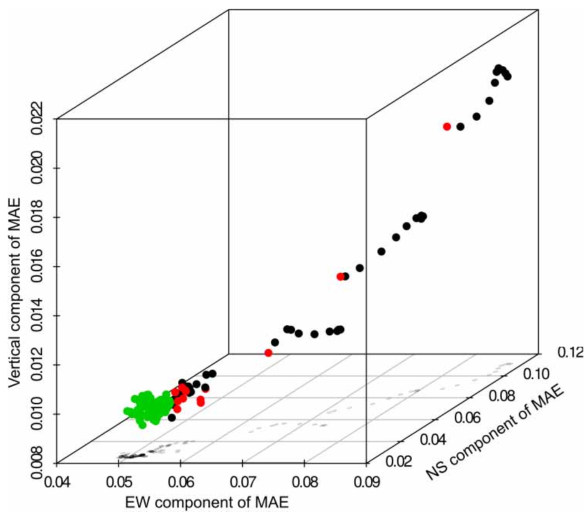

Figure 3. The three-dimensional scatterplot shows the EW, NS and vertical components of the cross-validation mean absolute error (MAE) for different combinations of S and T. Based on the 3D scatterplot, the projection of the points on the EW–NS plane is shown. See text for explanation.

of Figure 3 reveals the presence of clusters of points, with the most numerous cluster located near the origin of the 3D scatter plot. This larger cluster exhibits low values of the MAE for all the three components (EW, NS and vertical) of the representative unit vector. Further analysis revealed that points belong to three main groups, shown by different colours in Figure 3. The first group (dark points in Figure 3) includes points with $S \leq 1000$ m and $T > 10$. The second group (red points) encompasses points with $T = 10$ and the third group (green points) includes points with $S > 1000$ m and $T > 10$. The finding suggests that (at least in our study area) (1) individual BT segments should have a length of $S > 1000$ m and (2) the tension parameter should be $T > 10$ to obtain small MAE values. The use of $T \leq 10$ results in excessively smoothed BA surfaces that deviate considerably from the original measurement data points.

Figure 4 shows the distribution of the modulus of the MAE vectors, MAE_M (Table 1), constructed by combining the three components of the MAE (EW, NS and vertical). Only two points exhibit very low values of the modulus, corresponding to a $MAE_M < 0.062$, lower than the first percentile of the distribution (mean = 0.0664, median = 0.0658, 5th = 0.0630, 95th percentile = 0.0727, Figure 4). It is worth considering that the MAE provides a measure of the error along a given direction (EW, NS and vertical), whereas the MAE_M gives a comprehensive measure of the error. MAE_M is the modulus of the average vector difference between the vectors representing the original BAs information and those representing the interpolated

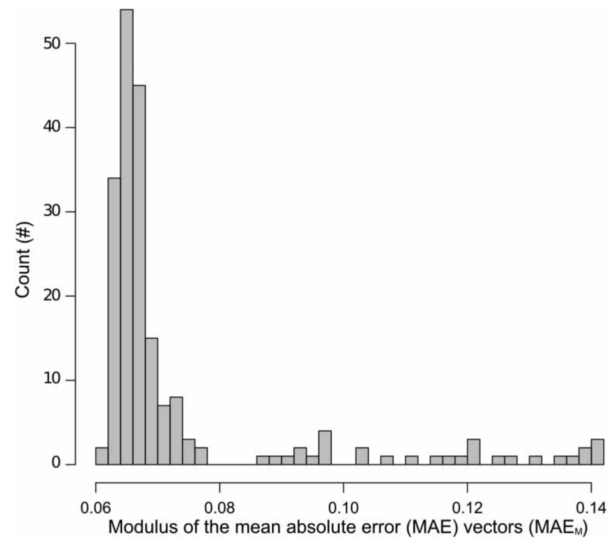

Figure 4. Histogram showing the distribution (frequency) of the modulus of the mean absolute error MAE vectors (MAE_M) obtained by combining the EW, NS and vertical components of the MAE. To prepare the histogram, only data pertaining to the cluster exhibiting small values for the MAE vector components (Figure 3) were selected.

Table 1. Performance of the geographical interpolation of the bedding attitude (BA) data measured by the modulus of the mean absolute error (MAE) vectors, MAE_M, and by the mean angular error (MA_NE).

MAE_M	MA_NE (°)	Segmentation length, S (m)	Tension, T
0.0615	3.52	2000	30
0.0618	3.54	2000	40
0.0621	3.56	2200	30
0.0624	3.58	2200	40
0.0629	3.60	2600	20
0.0629	3.60	2800	20
0.0629	3.60	3000	20

Note: Seven combinations for the tension parameter T and the segmentation length S that resulted in the smallest error vectors are listed.

BAs. We can show the mean angular error of the MAE_M, in angular degrees, as $MA_NE = 2 \times \arcsin(MAE_M / 2)$. When estimated for the combinations of the tension parameters T and S that have resulted in the smallest error vectors, MA_NE was always lower than 3.60° (Table 1). We conclude that using the "optimal" combinations of T and S, the interpolated BAs are very similar to those obtained using the BTs.

Further inspection of Figure 4 and Table 1 reveals that "optimal" results were obtained using a BT segment length $S > 2000$ m and values for the tension parameter $T \leq 40$, with the two best results obtained using $T = 30$ and $S = 2000$ m, and $T = 40$ and $S = 2000$ m. This suggests that only six of the original 207 BTs longer than 2000 m should be split. Consequently, in our study area the "optimal" set should contain 213 BTs. The figures are in good agreement with the values used by Santangelo et al. (2014) who, based on heuristic geomorphological considerations, split the original BTs into 223 segments and used a tension $T = 40$ for the interpolation. We emphasize that the number of segments is close to the "optimal" number of 213 BTs.

Figure 5 shows a comparison of the morpho-structural domains obtained for the "optimal" combination of the selected modelling parameters ($S = 2000$ m, $T = 30$, Figure 5(a)), and the domains prepared by Santangelo et al. (2014) adopting the heuristic geomorphological approach (Figure 5(b)).

Table 2 summarizes the two classifications and allows for a comparison of the abundance of landslides shown in the inventory map (Figure 1) in the two morpho-structural domains maps. Part I of Table 2 lists the percentages of the morpho-structural domains (A, O, C_O, C_D and C_U) covering (1) the entire study area (A_{TOT}), (2) the area not affected by old landslides (A_O) and (3) the area not affected by old or deep-seated landslides (A_{OD}). The percentages were calculated using the "optimal" combination of the selected modelling parameters and the heuristic approach. Part II of Table 2 lists the percentages of the morpho-structural domains (A, O, C_O, C_D, C_U) in landslide areas (A_{LT}) and (in brackets) the differences with the corresponding percentages listed in part I. The last column in Table 2 outlines the three considered landslide types (L_O, L_D and L_S).

In Table 2, negative values (in italics) indicate a lack of geographical association between landslides (of different types) and a given structural domain. Conversely, positive values indicate the association between landslides and a structural domain. The larger (smaller) the (absolute) difference, the stronger (weaker) is the geographical association. We infer that the difference in the proportion of landslide area is an indicator of the propensity to failures of a given bedding domain. A negative difference is indicative of a reduced propensity to generate slope failures, and a positive difference indicates a larger propensity to generate slope failures.

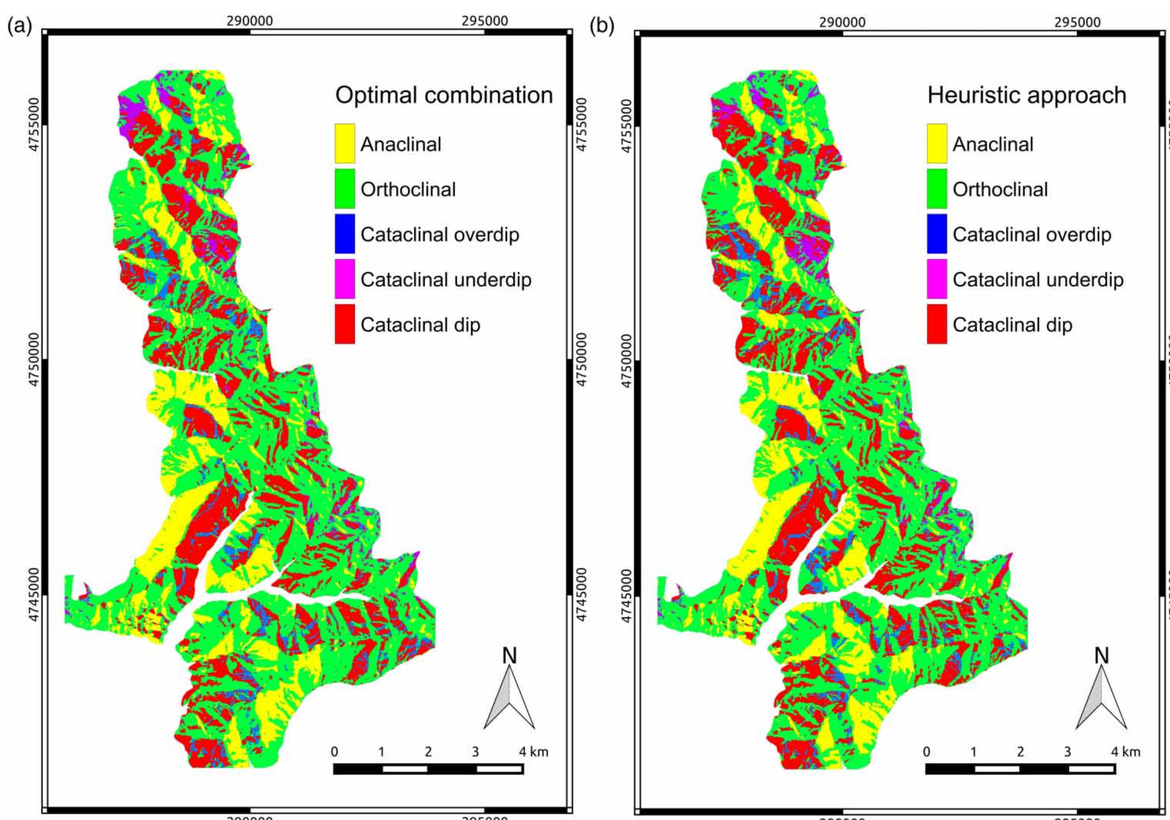

Figure 5. Morpho-structural domain maps obtained (a) using the "optimal" values for the tension $T = 30$ and the segmentation length $S = 2000$ m parameters, and (b) adopting a heuristic geomorphological approach to segment the BTs (Santangelo et al. 2014). The different colours show five different morpho-structural settings. UTM zone 33, datum ED50 (EPSG: 23033).

Table 2. Comparison of the extent of landslides of different types (L_O, old deep-seated landslides; L_D, deep-seated landslides; L_S, shallow landslides) and the extent of five morpho-structural settings (A, anaclinal; O, orthoclinal; C_O, cataclinal overdip; C_D, cataclinal dip; C_U, cataclinal underdip) determined using the "optimal" combination of the modelling parameters ($T = 30$, $S = 2000$ m, upper rows) and the heuristic geomorphological selection of the parameters proposed by Santangelo et al. (2014) (lower rows).

		I					II					
		A	O	C_O	C_D	C_U	A A_{LT} (Δ_A)	O A_{LT} (Δ_A)	C_O A_{LT} (Δ_A)	C_D A_{LT} (Δ_A)	C_U A_{LT} (Δ_A)	
Optimal parameters	A_{TOT}	17.2	51.2	4.9	23.8	2.9	9.2 (*–8.0*)	43.4 (*–7.8*)	2.6 (*–2.3*)	37.1 (13.3)	7.6 (4.8)	L_O
	A_O	17.5	51.5	5.0	23.3	2.7	10.7 (*–6.8*)	49.7 (*–1.8*)	8.2 (3.1)	29.0 (5.7)	2.4 (*–0.3*)	L_D
	A_{OD}	17.9	51.4	4.5	23.2	2.9	20.6 (2.7)	51.0 (*–0.3*)	7.4 (2.8)	18.2 (*–5.0*)	2.7 (*–0.2*)	L_S
Heuristic selection	A_{TOT}	17.4	49.8	5.2	24.8	2.8	13.2 (*–4.2*)	38.7 (*–11.1*)	2.4 (*–2.8*)	36.2 (11.4)	9.5 (6.7)	L_O
							14.7 (*–2.7*)	48.4 (*–1.5*)	7.4 (2.2)	27.0 (2.2)	2.5 (*–0.3*)	L_D
							19.5 (2.1)	51.2 (1.4)	7.8 (2.6)	19.1 (*–5.7*)	2.5 (*–0.3*)	L_S

Note: (I) Percentage of five morpho-structural domains for the entire study area (A_{TOT}), for the area not affected by old landslides (A_O) and for the area not affected by old or deep-seated landslides (A_{OD}). (II) Percentage of morpho-structural domains in landslide areas (A_{LT}), and difference (Δ_A) compared to (I). Legend: T, tension parameter. S, segmentation length (in meters). Negative values are shown in italics. See text for explanation.

Figure 6(I) compares the proportion of the different morpho-structural domains affected by landslides (A_{LT} in Table 2) in the inventory map (Figure 1) to the proportion of the structural domains in the entire study area (A_{TOT} in Table 2). In the figure, 0% means "no difference" between the proportion of a given morpho-structural domain in the entire study area and the same proportion in the areas covered by landslides. Positive (negative) values indicate greater (lesser) abundance of a specific morpho-structural domain in the areas where landslides are present, compared to the entire study area.

Inspection of the zonation obtained using the "optimal" combination of the modelling parameters ($T = 30$, $S = 2000$ m; Figure 6(I)) reveals that shallow landslides (L_S) are less abundant in the cataclinal dip (C_D) slope domain, and more abundant in the anaclinal (A) and the cataclinal overdip (C_O) slope domains. The deep-seated landslides (L_D) and the very old landslides (L_O) are less abundant in the anaclinal (A) and the orthoclinal (O) slope domains, and are more abundant in the cataclinal domains (C_O, C_D and C_U). In particular, the L_O are most abundant in the cataclinal dip (C_D) and the cataclinal underdip (C_U) domains, whereas the L_D are the most abundant in the cataclinal dip (C_D) and the cataclinal overdip (C_O) domains.

Figure 6 also allows for a comparison of the results obtained using the "optimal" parameters (Figure 6(I)) with the results obtained by Santangelo et al. (2014) adopting their heuristic approach to the selection of the parameters (Figure 6(II)). Although the results are similar, the "optimal" combination (Figure 6(I)) better emphasizes the abundance of L_O in the cataclinal dip (C_D) domain, and their relative scarcity in the anaclinal (A) slope domain. The abundance of L_O in the C_U slope domain can be attributed to the influence of bedding on the landslide occurrence, or it can be a misclassification problem resulting from a change in the local topography caused by the movement of the very large slope failures of the L_O type. The DEM used to outline the morpho-structural domains is more recent than the age of the L_O, and a lower slope angle determined by the landslides in their deposits should be considered and compared to the original topography. This suggests that the L_O were most probably triggered in C_D rather than in C_U bedding (structural) conditions, as incorrectly indicated by the analysis. This is in agreement with the indication that L_O in the study area, and more generally in Umbria, Central Italy, may have formed in climatic or seismic settings different from the present ones (Guzzetti and Cardinali 1990).

To perform the analysis shown in Figure 6(I), we excluded (1) all the shallow landslides (L_S) present on the top of pre-existing L_O and L_D, and (2) all deep-seated landslides (L_D) present on top of pre-existing L_O. We motivate the decision based on the following argument. Where an older (and typically larger) landslide exists, the large abundance of younger (and

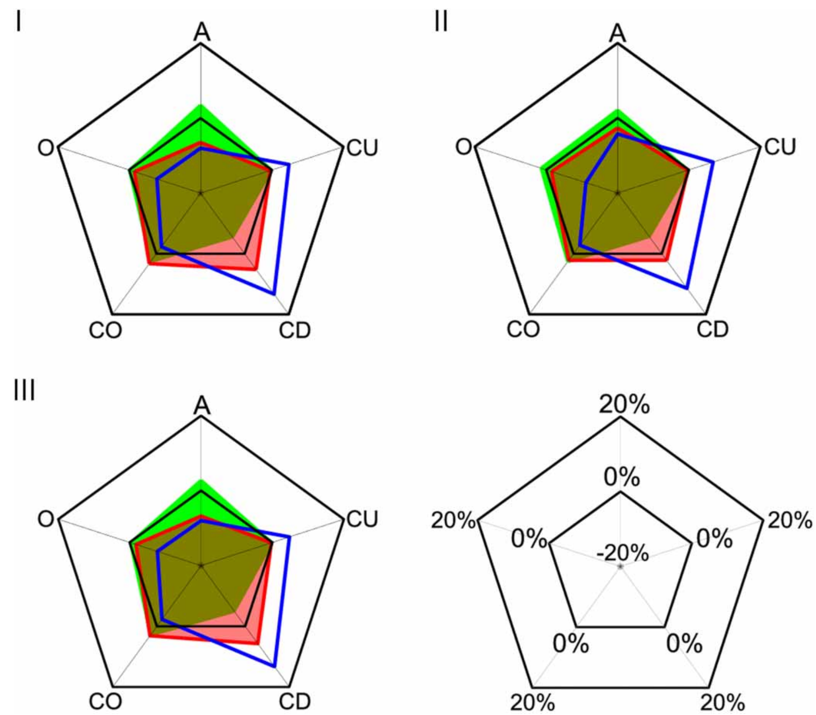

Figure 6. Spider charts show differences between the percentages of the five morpho-structural domains in areas with landslides, areas free of landslides and for the entire study area. Green polygons show differences for shallow landslides (L_S). Pink polygons show differences for deep-seated landslides (L_D). Blue lines show differences for old deep-seated landslides (L_O). (I) Comparison of differences between percentages in landslide areas (A_{LT}) and in the entire study area (A_{TOT}) using the "optimal" combination of the parameters (T = 30, S = 2000 m). (II) Same difference using the heuristic geomorphological approach adopted by Santangelo et al. (2014). (III) Comparison (difference, Δ_A in Table 2) for landslide areas and for landslide free areas (A_{TOT}, A_O and A_{OD} in Table 2), using the "optimal" combination of the parameters (T = 30, S = 2000 m). Legend: A, anaclinal slope; O, orthoclinal slope; C_O, cataclinal overdip slope; C_D, cataclinal dip slope; C_U, cataclinal underdip slope.

typically smaller) failures affecting the old landslide is attributed to the presence of the pre-existing landslide (a consequence of the reduced shear resistance of the failed materials) rather than to the original local structural setting that, in places, was altered by the occurrence of the older (and larger) landslide. To avoid a possible statistical bias (decrease) of L_S in the structural domains most affected by L_O and L_D, and a corresponding bias (increase) in the other domains, we compared the abundance of L_S in the five structural domains against the portion of the study area not affected by L_O and L_D (Figure 6(III)). For the comparison of the areas with and without landslides (Δ_A in Table 2), we considered (1) the entire study area (A_{TOT}) for the very old landslides (L_O), (2) the area not affected by very old landslides (A_O) for the deep-seated landslides (L_D), and the area not affected by very old (L_O) and by deep-seated (L_D) landslides (A_{OD}) for the shallow landslides (L_S).

Comparison of Figure 6(I) and 6(III) reveals that the exclusion of L_D and L_S overlaying older (pre-exiting) L_D and L_O did not influence the results significantly. The L_S are only slightly more abundant in the cataclinal overdip (C_O) and in the anaclinal (A) slope domains. We further observe that the relative abundance of L_S in the anaclinal (A) domain cannot be attributed to the local BA. The depth of the failure plane for the shallow landslide is less than 5 m in the study area, with a mean value of ~ 1.5 m (~1.0 m in agricultural areas; Fiorucci et al. 2011; Mergili et al. 2014c). We attribute the abundance of the L_S in the anaclinal (A) slope domain to the steepness of the local terrain (Table 3). In the study area, anaclinal (A) and cataclinal overdip (C_O) slopes are characterised by the presence of steep slopes (Santangelo et al. 2014), and we argue that the abundance of L_S in the two structural domains depends primarily on the steepness of the local terrain, and not on the geometry or the setting of the underlying bedrock.

5. Conclusions

We tested different combinations for the lengths S of BTs identified visually on stereoscopic aerial photographs, and for the values of the tension parameter T

Table 3. Distribution of the slope inclination values (in degrees) in the five morpho-structural domains computed using the "optimal" combination of the modelling parameters, $T = 30$, $S = 2000$ m.

Morpho-structural domain		Min (°)	Max (°)	Mean (°)	Std dev. (°)	25th (°)	50th (°)	75th (°)	90th (°)
Anaclinal	A	0	50.6	11.5	6.6	7.4	10.2	14.4	20.7
Orthoclinal	O	0	52.0	10.2	5.7	6.7	9.3	12.7	17.4
Cataclinal, overdip	C_O	1.6	40.8	15.9	4.7	12.6	14.8	18.2	22.4
Cataclinal, dip	C_D	0	21.1	7.1	3.5	4.8	7.1	9.4	11.8
Cataclinal, underdip	C_U	0	26.5	8.3	3.2	6.3	8.1	10.2	12.2

used for the geographical interpolation of the BA point data, to determine the influence of the two parameters on the reconstruction of BA maps. Our analysis indicates that the "optimal" parameters identified in this study through an iterative procedure are nearly identical to the parameters selected heuristically by expert geomorphologists (Santangelo et al. 2014). We conclude that an expert geomorphologist can select heuristically the "optimal" length of the BTs, and the "best" value for the interpolation parameter to exploit fully the BA information contained in the BTs. We further conclude that the cross-validation procedure adopted in this work to test the performance of the geographical interpolation of the available BA point measurements was capable of identifying the "optimal" combination of the modelling parameters. This opens to the possibility for a widespread extraction of accurate BA data, and the production of BA maps over large areas, from the automatic processing of BTs identified on stereoscopic aerial photographs or satellite images. Although we tested our method in a simple and regular lithological and structural setting, we maintain that the method can be applied in more complex settings, provided that the study area is divided into main structural domains bounded by, e.g. tectonic (faults, old axes) or stratigraphic (unconformities) discontinuities (Santangelo et al. 2014).

Exploiting the BA map and derivatives of a DEM, we produced a terrain zonation – using five morpho-structural domains – showing the geometrical relationships between the BA and the local slope, and we investigated the abundance of landslides of different types and sizes in the morpho-structural domains. The analysis confirmed the control exerted by the BA on the location and abundance of very-old deep-seated landslides (L_O) and on deep-seated landslides (L_D) in our study area.

We argue that BA should be considered when investigating the location and abundance of deep-seated landslides in layered rocks. The ability to prepare morpho-structural domains maps for large areas, exploiting information obtained rapidly from the visual interpretation of stereoscopic imagery, opens to the possibility of using structural information for regional susceptibility modelling. We expect that this will improve the quality of regional susceptibility models and associated terrain zonations (Galli et al. 2008).

Disclosure statement

No potential conflict of interest was reported by the authors.

Funding

MS and FB were supported by a grant of the Regione dell'Umbria under contract POR-FESR [Repertorio Contratti no. 861, 22/3/2012] and by a grant of the Italian National Department of Civil Protection.

ORCID

Ivan Marchesini http://orcid.org/0000-0002-8342-3134

References

Bodien, V., and J. C. Tipper. 2013. "An Image Analysis Procedure for Recognising and Measuring Bedding in Seemingly Homogeneous Rocks." *Sedimentary Geology* 284–285: 39–44. doi:10.1016/j.sedgeo.2012.11.002.

Bucci, F., M. Cardinali, and Guzzetti, F. 2013. "Structural Geomorphology, Active Faulting and Slope Deformations in the Epicentre Area of the MW 7.0, 1857, Southern Italy Earthquake." *Physics and Chemistry of the Earth* 63: 12–24.

Clegg, P., L. Bruciatelli, F. Domingos, R. R. Jones, M. De Donatis, and R. W. Wilson. 2006. "Digital Geological Mapping with Tablet PC and PDA: A Comparison." *Computers & Geosciences* 32 (10): 1682–1698. doi:10.1016/j.cageo.2006.03.007.

De Donatis, M., and Bruciatelli L. 2006. "MAP IT: The GIS Software for Field Mapping with Tablet Pc." *Computers & Geosciences* 32 (5): 673–680. doi:10.1016/j.cageo.2005.09.003.

De Kemp, E. A. 1998. "Three-dimensional Projection of Curvilinear Geological Features Through Direction Cosine Interpolation of Structural Field Observations." *Computers & Geosciences* 24 (3): 269–284.

Fiorucci, F., M. Cardinali, R. Carlà, M. Rossi, A. C. Mondini, L. Santurri, F. Ardizzone, and F. Guzzetti. 2011. "Seasonal Landslide Mapping and Estimation of Landslide Mobilization Rates Using Aerial and Satellite Images." *Geomorphology* 129 (1–2): 59–70. doi:10.1016/j.geomorph.2011.01.013.

Galli, M., F. Ardizzone, M. Cardinali, F. Guzzetti, and P. Reichenbach. 2008. "Comparing Landslide Inventory Maps." *Geomorphology* 94 (3–4): 268–289.

Goudie, A. 2004. *Encyclopedia of Geomorphology.* London: Routledge.

GRASS Development Team. 2015. *Geographic Resources Analysis Support System (GRASS) Software, version 6.4.0*. Open Source Geospatial Foundation. http://grass.osgeo.org.

Grelle, G., P. Revellino, A. Donnarumma, and F. M. Guadagno. 2011. "Bedding Control on Landslides: A Methodological Approach for Computer-Aided Mapping Analysis." *Natural Hazards and Earth System Science* 11: 1395–1409.

Günther, A. 2003. "SLOPEMAP: Programs for Automated Mapping of Geometrical and Kinematical Properties of Hard Rock Hill Slopes." *Computers & Geosciences* 29: 865–875.

Guzzetti, F., F. Ardizzone, M. Cardinali, M. Rossi, and D. Valigi. 2009. "Landslide Volumes and Landslide Mobilization Rates in Umbria, Central Italy." *Earth and Planetary Science Letters* 279 (3–4): 222–229. doi:10.1016/j.epsl.2009.01.005.

Guzzetti, F., and M. Cardinali. 1990. "Landslide Inventory Map of the Umbria Region, Central Italy." Proceedings VI ICFL – ALPS 90, Milan, 12 September 1990, 273–284.

Guzzetti, F., M. Cardinali, and P. Reichenbach. 1996. "The Influence of Structural Setting and Lithology on Landslide Type and Pattern." *Environmental & Engineering Geoscience* 2 (4): 531–555.

Guzzetti, F., M. Galli, P. Reichenbach, F. Ardizzone, and M. Cardinali. 2006. "Landslide Hazard Assessment in the Collazzone Area, Umbria, Central Italy." *Natural Hazards and Earth System Science* 6: 115–131. doi:10.5194/nhess-6–115-2006.

Hofierka, J., T. Cebecauer, and M. Šúri. 2007. "Optimisation of Interpolation Parameters Using Cross-validation." In *Digital Terrain Modelling*, 67–82. Berlin: Springer. doi:10.1007/978–3-540-36731-4_3.

Hofierka, J., J. Parajka, H. Mitasova, and L. Mitas. 2002. "Multivariate Interpolation of Precipitation Using Regularized Spline with Tension." *Transactions in GIS* 6 (2): 135–150.

Keaton, J. R., and J. V. DeGraff. 1996. "Surface Observation and Geologic Mapping." In *Landslides, Investigation and Mitigation*. Transportation Research Board Special Report 247, edited by A. K. Turner and R. L. Schuster, 178–230. Washington, DC: National Academy Press.

Lisle, R. J. 1996. *Geological Structures and Maps: A Practical Guide*. Oxford: Butterworth-Heinemann.

Marchesini, I., M. Mergili, M. Rossi, M. Santangelo, M. Cardinali, F. Ardizzone, and F. Guzzetti. 2014. "A GIS Approach to Analysis of Deep-Seated Slope Stability in Complex Geology." In *Landslide Science for a Safer Geoenvironment*, edited by K. Sassa, P. Canuti, Y. Yin, 2, 483–489. doi:10.1007/978-3-319-05050-8.

Marchesini, I., M. Santangelo, F. Fiorucci, M. Cardinali, M. Rossi, and F. Guzzetti. 2013. "A GIS Method for Obtaining Geologic Bedding Attitude." In edited by C. Margottini, P. Canuti, and K. Sassa, Vol. 1, 243–247. Berlin, Heidelberg: Springer. doi:10.1007/978-3-642-31325-7.

Meentemeyer, R. K., and A. Moody. 2000. "Automated Mapping of Conformity Between Topographic and Geological Surfaces." *Computers & Geosciences* 26 (7): 815–829.

Mergili, M., I. Marchesini, M. Alvioli, M. Metz, B. Schneider-Muntau, M. Rossi, and F. Guzzetti. 2014a. "A Strategy for GIS-Based 3-D Slope Stability Modelling Over Large Areas." *Geoscientific Model Development* 7: 2969–2982. www.geosci-model-dev.net/7/2969/2014/. doi:10.5194/gmd-7-2969-2014.

Mergili, M., I. Marchesini, M. Alvioli, M. Rossi, M. Santangelo, M. Cardinali, W. Fellin, and F. Guzzetti. 2014b. "GIS-Based Deterministic Analysis of Deep-Seated Slope Stability in a Complex Geological Setting." In *Engineering Geology for Society and Territory - Volume 2*, edited by G. Lollino, D. Giordan, G. B. Crosta, J. Corominas, R. Azzam, J. Wasowski, and N. Sciarra, Vol. 2, 1437–1441. Cham: Springer. doi:10.1007/978-3-319-09057-3.

Mergili, M., I. Marchesini, M. Rossi, F. Guzzetti, and W. Fellin. 2014c. "Spatially Distributed Three-Dimensional Slope Stability Modelling in a Raster GIS." *Geomorphology* 206: 178–195. ISSN 0169-555X. doi:10.1016/j.geomorph.2013.10.008.

Mitášová, H., L. Mitášm, R. S. Harmon. 2005. "Simultaneous Spline Approximation and Topographic Analysis for Lidar Elevation Data in Open-Source GIS." *IEEE Geoscience and Remote Sensing Letters* 2 (4): 375–379.

Neteler, M., and H. Mitášová. 2008. *Open Source GIS: A GRASS GIS Approach*. 3rd ed. New York: Springer, 426.

Santangelo, M., I. Marchesini, M. Cardinali, F. Fiorucci, M. Rossi, F. Bucci, and F. Guzzetti. 2014. "A Method for the Assessment of the Influence of Bedding on Landslide Abundance and Types." *Landslides* (August 2013). doi:10.1007/s10346-014-0485-x.